

Large Bychkov-Rashba spin-orbit coupling in high mobility GaN/AlGaN heterostructures

S. Schmult¹, M. J. Manfra^{1,*}, A. Punnoose^{1,2}, A. M. Sergent¹, K. W. Baldwin¹, and R. J. Molnar³

¹*Bell Laboratories, Lucent Technologies, 700 Mountain Avenue, Murray Hill, New Jersey 07974, USA*

²*Physics Department, University of Wisconsin, 11500 University Ave., Madison, WI 53706, USA*

³*MIT Lincoln Laboratory, 244 Wood St., Lexington, Massachusetts 02420, USA*

We present low temperature magnetoconductivity measurements of a density-tunable and high mobility two-dimensional electron gas confined in the wide bandgap GaN/AlGaN system. We observed pronounced anti-localization minima in the low-field conductivity, indicating the presence of strong spin-orbit coupling. Density dependent measurements of magnetoconductivity indicate that the coupling is mainly due to the Bychkov-Rashba mechanism. In addition, we have derived a closed-form expression for the magnetoconductivity, allowing us to extract reliable transport parameters for our devices. The Rashba spin-orbit coupling constant is $\alpha_{so} \sim 6 \times 10^{-13} \text{eVm}$, while the conduction band spin-orbit splitting energy amounts to $\Delta_{so} \sim 0.3 \text{meV}$ at $n_e = 1 \times 10^{16} \text{m}^{-2}$.

GaN has emerged as a leading material for a variety of new device applications, ranging from solid-state, ultra-violet optical sources to high power electronics [1]. While the performance of many devices fabricated from GaN has been stunning, several fundamental physical processes remain to be understood. A prime example is spin-orbit coupling in GaN and its heterostructures. The burgeoning field of spintronics has invigorated the study of spin-orbit coupling in semiconducting materials [2, 3]. To date, much experimental effort has been devoted to narrow bandgap material systems (InAs, InGaAs, GaAs, etc) as spin-orbit coupling is expected to be strong in these systems. Conversely, far less experimental effort has been directed toward wide bandgap systems like GaN in which spin-orbit effects are predicted to be suppressed by the large fundamental bandgap, E_g , and reduced spin-orbit splitting, Δ_0 , of the valence band at zone center. Indeed, in the $\mathbf{k}\cdot\mathbf{p}$ formalism [4], the bare Rashba spin-orbit coupling constant for electrons, α_0 , scales as: $\alpha_0 \sim \Delta_0/E_g^2$. As the value of Δ_0 for GaAs exceeds that of GaN by a factor of 30, it is reasonable to suspect that spin splitting of the conduction band in GaN-based heterostructures would be insignificant compared to GaAs and other narrow gap heterostructures.

Spin-orbit coupling for conduction band electrons in *bulk* GaN was considered by Krishnamurthy [5] who calculated that the spin relaxation times in bulk GaN should exceed the spin relaxation time in GaAs by *three orders of magnitude*, thus making GaN an excellent candidate for transport of spin polarized currents over macroscopic distances. However, in Ref. [5] GaN was assumed to have the zinc-blende lattice structure. GaN is typically grown in the more stable wurtzite phase. It is known that the symmetry of the underlying crystal has a profound impact on spin-orbit induced splittings in the conduction band [6, 7]. While the work of Ref. [5] is suggestive, very few experimental results for bulk wurtzite GaN have been reported [8] and the impact of spin-orbit coupling on transport in wurtzite GaN/AlGaN heterostructures remains an open question. A few preliminary experi-

ments have considered spin-orbit coupling for the two-dimensional electron gas (2DEG) [9, 10, 11, 12] in a narrow parameter space of high density and low mobility. The influence of spin-orbit coupling in the limit of low 2DEG density and high mobility has not been addressed. Furthermore, probative experiments in which conductivity is tuned over a broad range, and theoretical analysis specifically tailored to the physics of GaN are needed to understand the mechanisms of spin-orbit coupling and accurately quantify spin-orbit effects in high mobility GaN 2DEGs.

In this Letter we present an analysis of low temperature magnetoconductivity measurements in a series of high mobility 2DEGs confined in the wide bandgap GaN/AlGaN system. Experiments are conducted with gated Hall bars that allow access to a previously inaccessible range of low density, $5 \times 10^{15} \text{m}^{-2} \leq n_e \leq 1.8 \times 10^{16} \text{m}^{-2}$, and very high mobilities $1.4 \text{m}^2/\text{Vs} \leq \mu \leq 8.7 \text{m}^2/\text{Vs}$. We observe non-monotonic behavior in the magnetoconductivity with a pronounced antilocalization minimum at $B \sim 2 \text{mT}$, indicating the presence of significant spin-orbit coupling. In addition, we have derived an exact closed-form expression for the magnetoconductivity, that allows for the extraction of reliable spin-orbit parameters relevant to our devices. The relative simplicity of the formula for the magnetoconductivity greatly facilitates data fitting. Importantly, the magnetic field at which the magnetoconductivity minimum occurs does not depend sensitively on electron density. As we shall show, this result implies that the Bychkov-Rashba mechanism is the dominant spin-orbit coupling in our samples. The extracted Rashba coupling constant $\alpha_{so} = 6 \times 10^{-13} \text{eVm}$ is large, resulting in spin-split energies ranging from 0.2meV to 0.4meV within the density range of our experiment. The value of α_{so} in GaN is comparable to that seen in the narrower bandgap GaAs system. Our findings place severe constraints on the use of GaN heterostructures for polarized spin transport, but also suggest that GaN may be implemented in applications where only narrow bandgap materials have been

considered previously.

Magnetoconductivity in two dimensions has been studied extensively in the diffusive limit [13, 14]. The conductivity of a 2DEG in classically weak magnetic fields, $\sigma(B)$, shows signatures of quantum interference that depend on the magnetic field and spin-orbit coupling. Spin relaxation due to spin-orbit coupling and impurity scattering produces a positive contribution to the conductivity known as antilocalization. Magnetic field suppresses this antilocalization. The functional dependence of $\Delta\sigma(B)$, where $\Delta\sigma(B) = \sigma(B) - \sigma(B=0)$, at small magnetic fields depends on the relative contributions of dephasing (characterized by a dephasing rate $1/\tau_\varphi$) and the spin-relaxation rate given by $1/\tau_{so}$. Strong spin relaxation compared to dephasing leads to a pronounced minimum in the magnetoconductivity for excursions away from $B=0$. The observation of an antilocalization minimum in the magnetoconductivity is the signature of spin-orbit coupling.

The Bychkov-Rashba interaction in a 2D system can be described by the following Hamiltonian [15]:

$$H = \frac{\vec{p}^2}{2m} + \alpha_{so} \vec{\sigma} \cdot (\hat{z} \times \vec{p}). \quad (1)$$

Here, α_{so} is the spin-orbit coupling strength, the split-

ting energy is $\Delta_{so}=2\alpha_{so}p_F$ (at the Fermi surface). In a 2D system with spin-orbit interactions, the dominant spin relaxation process is typically the D'yakonov-Perel' (DP) mechanism [16]. It describes the relaxation of the electron spin in the presence of a spin-splitting, Δ_{so} . Relaxation occurs because the direction of the axis of spin precession is tied to the direction of the electron momentum, which changes randomly with each collision. As a result, the net precession after N collisions is typically $\sqrt{N}\Delta_{so}\tau/\hbar$ in the diffusive transport regime, where τ is the mean free time. Consequently, the time it takes to randomize the spin is $\tau_{so} \sim \hbar^2/\Delta_{so}^2\tau$. Expressed in terms of α_{so} , $1/\tau_{so}=D(2m\alpha_{so}/\hbar)^2$, where $D = v_F^2\tau/2$ is the diffusion constant in 2D.

We analyze the measured magnetoconductivity data with an analytical formula we have derived for $\Delta\sigma(B)$ in the presence of the Bychkov-Rashba interaction that is valid in the diffusive regime. The details of our derivation are presented in an upcoming publication [17]. This formulation greatly simplifies extraction of the transport parameters from experimental data. The relevant magnetic field scales are: $B_{so} = \hbar/4eD\tau_{so}$, $B_\varphi = \hbar/4eD\tau_\varphi$, and $B_{tr}=\hbar/4eD\tau$. The diffusive limit is defined as $B \ll B_{tr}$. In this limit, $\Delta\sigma(B)$ is independent of B_{tr} and the expression for $\Delta\sigma(B)$ reads:

$$\Delta\sigma(B) = \frac{e^2}{2\pi h} \left[\sum_{s=0,\pm 1} u_s \psi \left(\frac{1}{2} + b_\varphi - v_s \right) - \psi \left(\frac{1}{2} + b_\varphi \right) + \frac{1}{(b_{so} + b_\varphi)^2 - 1/4} - 2 \ln b_\varphi + C \right], \quad (2)$$

$$C = -2 \ln \left(1 + \frac{B_{so}}{B_\varphi} \right) - \ln \left(1 + \frac{2B_{so}}{B_\varphi} \right) + \frac{8}{\sqrt{7 + 16B_\varphi/B_{so}}} \arccos \left[\frac{2B_\varphi/B_{so} - 1}{\sqrt{(2B_\varphi/B_{so} + 3)^2 - 1}} \right]. \quad (3)$$

The values of u_s and v_s are:

$$v_s = 2 \delta \cos \left[\theta - \frac{2\pi}{3}(1-s) \right], \quad (4)$$

$$u_s = \frac{3v_s^2 + 4b_{so}v_s + (5b_{so}^2 + 4b_{so}b_\varphi - 1)}{\prod_{s' \neq s} (v_s - v_{s'})}, \quad (5)$$

where the variables δ and θ are equal to:

$$\delta = \sqrt{\frac{1 - 4b_{so}b_\varphi - b_{so}^2}{3}}, \quad (6)$$

$$\theta = \frac{1}{3} \arccos \left[- \left(\frac{b_{so}}{\delta} \right)^3 \left(1 + \frac{2b_\varphi}{b_{so}} \right) \right]. \quad (7)$$

$\psi(z)$ is the di-gamma function, while $b_{so}=B_{so}/B$ and $b_\varphi=B_\varphi/B$. The constant C is such that $\Delta\sigma(0) = 0$. Eq. (2) provides an analytical, closed-form, solution for the magnetoconductivity in the presence of the

Bychkov-Rashba interaction. The result is expressed in terms of the two parameters B_{so} and B_φ . Because, $B_{so} = (m\alpha_{so})^2/e\hbar$, determining B_{so} as a fitting parameter gives, if the mass is known, directly the value of the spin-orbit coupling α_{so} defined in Eq. (1).

The samples used in this study are single interface GaN/AlGaN heterostructures grown by plasma-assisted molecular beam epitaxy (MBE) on (0001) oriented GaN templates. After an initial 1 μ m GaN buffer layer, a 16nm thick $\text{Al}_x\text{Ga}_{1-x}\text{N}$ barrier layer (x varies between 0.08 and 0.12) is grown followed by a 3nm thick GaN capping layer. The 2DEG is formed at the lower GaN/AlGaN interface without modulation doping due to the effects of spontaneous and piezoelectric polarization [18]. Hall bars with 100 μ m width and 2mm length are defined with 14 voltage probes symmetrically placed along the device. A Ni/Au gate, separated by 50nm of SiO_2 from the wafer

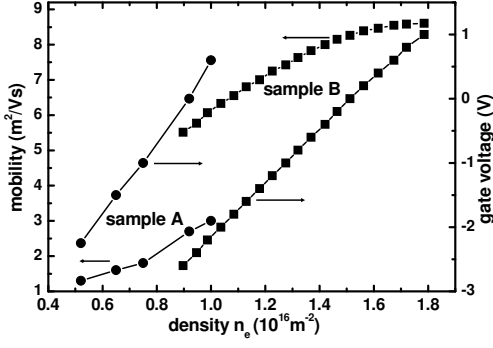


FIG. 1: Transport parameters of our gated Hall bar devices. Sample A (solid black circles) has lower conductivity, placing it in the diffusive transport regime. Sample B (solid black squares) is a high mobility device. The combination of the two devices allows access to a broad range of 2D conductivity.

surface, is used to control the 2DEG density. The magnetic field dependent conductivity was measured with standard low frequency lock-in techniques at $T=0.3\text{K}$. All investigated samples show an unambiguous minimum in low field magnetoconductivity, indicative of strong spin-orbit coupling.

We discuss in detail two samples with different conductivity (see Fig. 1). The first structure, sample A, is designed to have a mobility and carrier density which place it in the diffusive limit at low carrier density. With Sample A, we are able to tune the conductivity from the diffusive limit, where our theory is strictly valid and the extracted parameters are most accurate, to the ballistic regime at higher carrier density. Our objective is to extract reliable parameters for sample A in the diffusive limit and then monitor the evolution of the magnetoconductivity as the transport moves into the ballistic regime. Sample B, which has $\mu = 8.7\text{m}^2/\text{Vs}$ at $n_e = 1.8 \times 10^{16}\text{m}^{-2}$, is a very high mobility sample [21, 22] which extends our study deep into the ballistic regime.

The experimentally obtained data are plotted as a change in conductivity $\Delta\sigma(B) = \sigma(B) - \sigma(B=0)$ and are shown in Fig. 2 for sample A. We note that Eq. (2) predicts a crossover field from negative magnetoconductivity to positive magnetoconductivity at $B \approx B_{so}$. Several features are evident in the data. While we change the density by a factor of two and the conductivity by a factor of four, the field scale at which the magnetoconductivity minimum occurs does not change within our experimental accuracy. This fact has two immediate consequences. As the magnitude of the spin-orbit coupling constant α_{so} is directly proportional to B_{so} , the data implies that the Bychkov-Rashba coupling strength does not change as a function of density. In addition, the lack of field dependence of the conductivity minimum justifies our neglect of the linear and cubic Dresselhaus terms in the model Hamiltonian, since the presence of Dresselhaus coupling dictates that the field scale B_{so} acquires an explicit den-

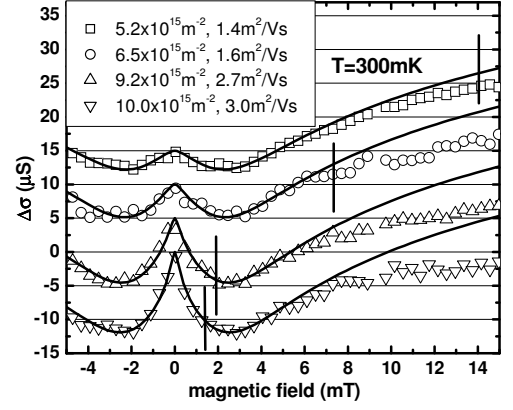


FIG. 2: Measured magnetoconductivity data (symbols) of sample A for small magnetic fields over a wide range of density and mobility (inset). In all cases $\Delta\sigma(B=0) = 0$. The traces have been shifted for clearer presentation. The solid lines denote the fit of Eq. (2) at each density. The vertical bars are at the position of B_{tr} , denoting the limit to the diffusive regime.

sity dependence, $B_{so} \sim \gamma^2 n_e^2$ [19, 20].

We also see that while the magnetic field position of the conductivity minimum does not change with conductivity, the amplitude of the antilocalization effect does. The antilocalization induced drop in conductivity is largest at highest conductivity while it is suppressed at lower conductivity. Since the field scale of the conductivity minimum, B_{so} , is largely constant, the reduction in the amplitude of the antilocalization behavior can be attributed to the change in B_ϕ as the density and mobility are reduced.

Using the model presented earlier, the changes to the conductivity due to quantum interference in the presence of spin-orbit coupling at each density were calculated (solid lines in Fig. 2), allowing for the extraction of B_{so} and B_ϕ . Also shown by vertical lines are the values of B_{tr} for each density. As expected, the deviation of the fits from the data becomes significant at fields $B \sim B_{tr}$.

The values for B_{so} and B_ϕ extracted from the magnetoconductivity are plotted as a function of 2DEG density in Fig. 3. The field scale B_ϕ associated with dephasing decreases its value as the conductivity increases. The values for B_ϕ correspond to a dephasing time $\tau_\phi \sim 100\text{ps}$ in sample A. As could be expected from inspection of the raw data, B_{so} remains at $\sim 2\text{mT}$ for the whole range of densities explored. The corresponding values for the spin dephasing time τ_{so} vary from 2ps (high density) to 10ps (low density). Using $B_{so} \sim 2\text{mT}$, the spin-orbit coupling parameter $\alpha_{so} = 6 \times 10^{-13}\text{eV}\text{m}$ is calculated, yielding a density dependent splitting, Δ_{so} , of the two spin subbands at the Fermi edge of $0.2\text{meV} - 0.3\text{meV}$ for this sample.

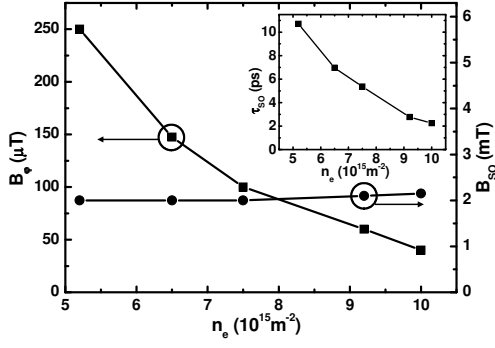


FIG. 3: The density dependent values of B_{so} and B_{φ} extracted from the fits in Fig. 2. While B_{φ} decreases by a factor of six with increasing density, B_{so} shows little density dependence. The inset shows the evolution of τ_{so} as a function of 2D density.

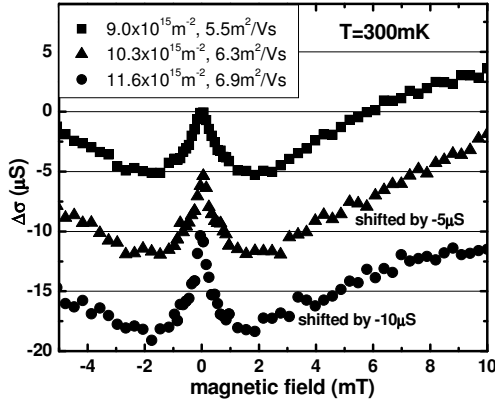


FIG. 4: Magnetoconductivity data for sample B. The high mobility of sample B dictates that the transport is ballistic. As with sample A, the conductivity minimum is situated near $B=2\text{mT}$ and does not depend significantly on 2D density.

We now turn to sample B. In sample B, B_{tr} covers the range between $100\mu\text{T}$ and $440\mu\text{T}$ and is thus significantly smaller than the field scale B_{so} . It is clear from the forgoing discussion that our closed form expression for the magnetoconductivity has limited applicability in this regime. We therefore do not attempt to fit the data. Nevertheless, we still can glean important information from the raw data. The magnetoconductivity data for sample B are presented in Fig. 4. The conductivity minimum does not change position with density and the minimum conductivity is again near $B=2\text{mT}$, as in sample A. It follows that the value of α_{so} for sample B will be approximately the same as in sample A. Indeed, it is not surprising that B_{so} has not changed significantly in moving from sample A to sample B as the layer sequence of the two

structures is nearly identical. Given a maximum density $n_e=1.8\times 10^{16}\text{m}^{-2}$, a zero field spin splitting of 0.4meV is calculated for sample B. It is interesting to compare our value of spin splitting to the results of Chou *et al.* [23] who examined the zero-field splitting observed in quantum point contacts (QPC) fabricated on a similar high mobility GaN heterostructure. In a QPC built on a GaN 2DEG with $n_e=1\times 10^{16}\text{m}^{-2}$ and $\mu=5.6\text{m}^2/\text{Vs}$, Chou observed a zero-field splitting of 0.39meV , a result which compares favorably with our value determined from magnetoconductivity measurements of a GaN 2DEG.

The origin of the large Bychkov-Rashba coupling in GaN heterostructures is yet to be fully explained. One possible explanation is found in the extremely large electric fields at the AlGaIn/GaN interface generated by the polarization discontinuity. Self-consistent calculations suggest that the electric field in our GaN heterostructure with $n_e=5\times 10^{15}\text{m}^{-2}$, is approximately 10 times the value in an equivalent density GaAs 2DEG structure [24]. Since $\alpha_{so}=\alpha_0 E$, where α_0 is the fundamental spin-orbit coupling parameter for a particular material system and E is the value of the electric field at the heterointerface, it may be that large zero-field spin splitting is due to the large increase in electric field. It is also possible that the fundamental spin-orbit coupling may be enhanced in wurtzite GaN due to coupling between the conduction band and higher energy conduction bands. A calculation of α_0 in GaN which accounts for the wurtzite symmetry and includes remote band effects is still lacking. While further study is needed, our experiments clearly indicate that spin-orbit coupling dramatically influences the transport properties of high mobility GaN 2DEGs.

*Corresponding author: manfra@lucent.com

- [1] For a review see, *Nitride Semiconductors and Devices*, H. Morkoc, Springer (1999)
- [2] S. Datta and B. Das, Appl. Phys. Lett. **56**, 665 (1990).
- [3] I. Zutic, J. Fabian, and S. Das Sarma, Rev. Mod. Phys. **76**, 323 (2004).
- [4] M. Cardona, N. E. Christensen, and G. Fasol, Phys. Rev. B **38**, 1806 (1988).
- [5] S. Krishnamurthy, M. van Schilfgaarde, and N. Newman, Appl. Phys. Lett. **83**, 1761 (2003).
- [6] E. I. Rashba, Sov. Phys. Solid State **2**, 1109 (1960)
- [7] L. C. Lew Yan Voon, M. Willatzen, M. Cardona, and N. E. Christensen, Phys. Rev. B, **53**, 10703 (1996).
- [8] B. Beschoten, E. Johnston-Halperin, D. K. Young, M. Poggio, J. E. Grimaldi, S. Keller, S. P. DenBaars, U. K. Mishra, E. L. Hu, and D. D. Awschalom, Phys. Rev. B **63**, 121202 (2001).
- [9] Ikai Lo, T. K. Tsai, W. J. Yao, P. C. Ho, Li-Wei Tu, T. C. Chang, S. Elhamri, W. C. Mitchel, K. Y. Hsieh, J. H. Huang, H. L. Huang, and Wen-Chung Tsai, Phys. Rev. B **65**, 161306 (2002).
- [10] J. Lu, B. Shen, N. Tang, D. J. Chen, H. Zhao, D. W. Liu, R. Zhang, Y. Shi, Y. D. Zheng, Z. J. Qiu, Y. S. Gui, B. Zhu, W. Yao, J. H. Chu, K. Hoshino, and Y. Arakawa,

- Appl. Phys. Lett. **85**, 3125 (2004).
- [11] W. Weber, S. D. Ganichev, S. N. Danilov, D. Weiss, W. Prettl, Z. D. Kvon, H. Cho, and J. Lee, Appl. Phys. Lett. **87**, 262106 (2005).
 - [12] N. Thillozen, Th. Schäpers, N. Kaluza, H. Hardtdegen, and V.A. Guzenko, Appl. Phys. Lett. **88**, 022111 (2006).
 - [13] S.V. Iordanskii, Y.B. Lyanda-Geller, and G.E. Pikus, JETP Lett. **60**, 207 (1994).
 - [14] V. M. Edelstein, J. Phys.: Condensed Matter **7**, 1 (1995)
 - [15] Y.A. Bychkov, and E.I. Rashba, JETP Lett. **39**, 78 (1984)
 - [16] M.I. D'yakonov, and V.I. Perel', Sov. Phys. Solid State **13**, 3023 (1972).
 - [17] A. Punnoose, accepted for publication in Appl. Phys. Lett.
 - [18] O. Ambacher, J. Smart, J. R. Shealy, N. G. Weimann, K. Chu, M. Murphy, W. J. Schaff, L. F. Eastman, R. Dimitrov, L. Wittner, M. Stutzmann, W. Rieger, and J. Hilsenbeck, J. Appl. Phys. **85**, 3222 (1999).
 - [19] J.B. Miller, D.M. Zuhmbühl, C.M. Marcus, Y.B. Lyanda-Geller, D. Goldhaber-Gordon, K. Campman, and A.C. Gossard, Phys. Rev. Lett. **90**, 076807 (2003).
 - [20] W. Knap, C. Skierbiszewski, A. Zduniak, E. Litwin-Staszewska, D. Bertho, F. Kobbi, J. L. Robert, G. E. Pikus, F. G. Pikus, S. V. Iordanskii, V. Mosser, K. Zekentes, and Yu. B. Lyanda-Geller, Phys. Rev. B **53**, 3912 (1996).
 - [21] M. J. Manfra, K. W. Baldwin, A. M. Sergent, R. J. Molnar, and J. Caissie, Appl. Phys. Lett. **85**, 1722 (2004).
 - [22] M. J. Manfra, K. W. Baldwin, A. M. Sergent, K. W. West, R. J. Molnar, and J. Caissie, Appl. Phys. Lett. **85**, 5394 (2004).
 - [23] H.T. Chou, S. Luscher, D. Goldhaber-Gordon, M. J. Manfra, A. M. Sergent, K. W. West, and R. J. Molnar, Appl. Phys. Lett. **86**, 073108 (2005).
 - [24] B. Jogai, J. Appl. Phys. **91**, 3721 (2002).